Supplementary Materials

CREB1 spatio-temporal dynamics within the rat pineal gland

Luz E. Farias Altamirano[1], Elena Vásquez[1], Carlos L. Freites[1], Jorge E. Ibañez[1], Mario E. Guido[2] and Estela M. Muñoz[1*]

Table S1. CREB1 distribution within individual pinealocyte nuclei.

Nuclear pixels positive for CREB1 (% of the total nuclear pixels)							
ZT or Surgical condition	**N (Pineal glands)**	**Nu (Pinealocyte nuclei)**	**Mean**	**SD**	**SEM**	**Statistics***	
ZT6	4	232	21.342	7.803	0.512	0.0001	D
ZT10	4	231	26.53	7.208	0.474		C
ZT14	3	119	35.61	12.41	1.14		A
ZT18	3	174	30.485	10.331	0.783		B
SCGx (ZT14)	4	122	37.07	11.79	1.07	0.0001	A
SHAM (ZT14)	4	109	24.591	7.776	0.745		B

*SCGx: superior cervical ganglionectomy; SEM: standard error of the mean; SD: standard deviation; SHAM: sham surgery; ZT: Zeitgeber time; *: one-way ANOVA followed by the Tukey post-test. Different letters indicate $p < 0.01$ vs. each other.*

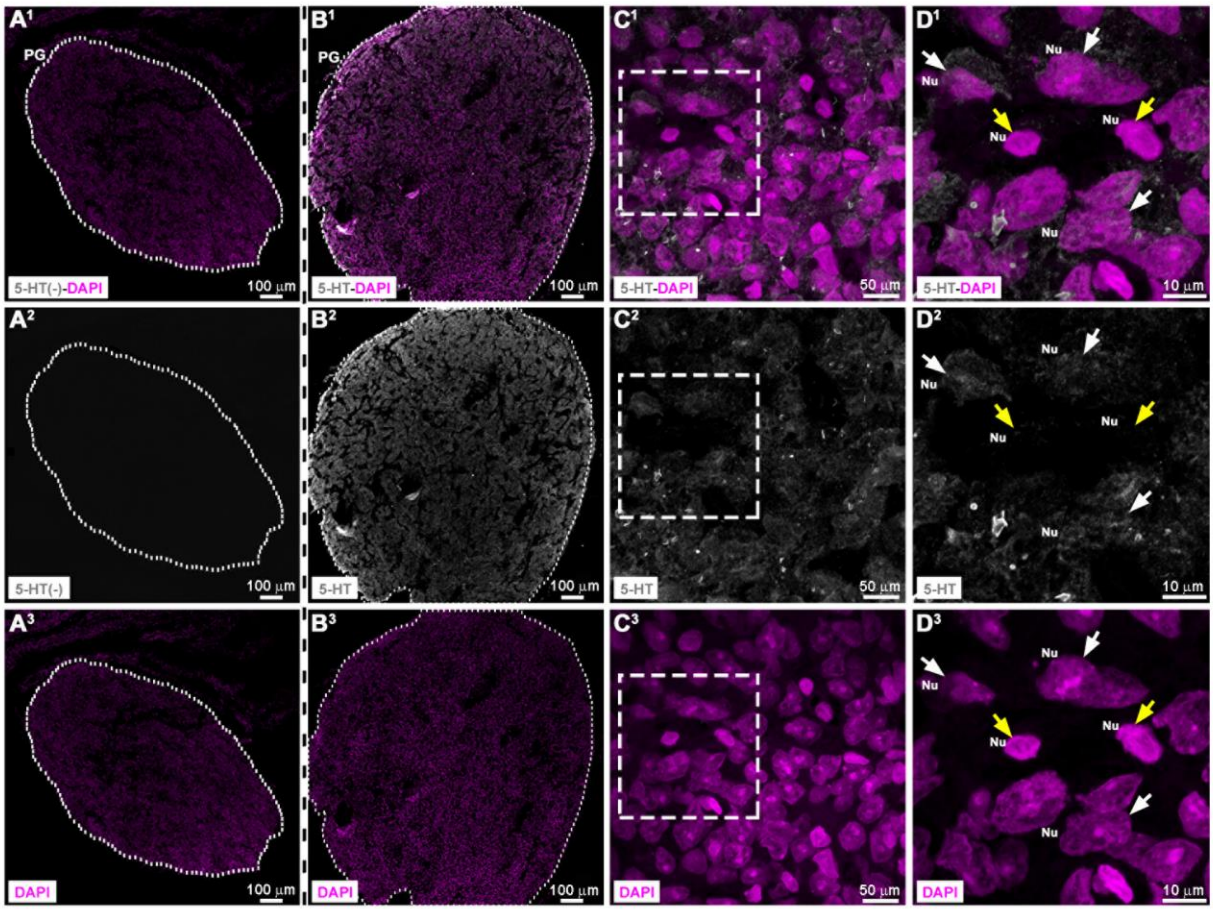

Fig. S1. Identification of pinealocytes within the rat pineal gland.

Section of adult rat pineal gland (PG) collected at ZT6 and immunolabeled for the melatonin precursor, 5-hydroxytryptamine (5-HT; grey). Nuclei (Nu) were stained with 4',6-diamidino-2-phenylindole (DAPI; magenta). (A^1-A^3) Negative control by omission of the anti-5-HT antibody. (B^1-D^3) PG section in the presence of the primary antibody and/or the nuclear dye. (A^1-B^3) 10x images; scale bar: 100 µm. The PG perimeter is defined by a dashed white line. (C^1-C^3) 2x digital zooms from 60x images; scale bar: 50 µm. (D^1-D^3) 2.5x digital zooms from 100x images of the insets shown in C^1-C^3; scale bar: 10 µm. Predominant pinealocytes are easily identified due to their nuclear architecture and their immunoreactivity for 5-HT (white arrows). Non-pinealocyte cells with homogenous and compact chromatin showed no signal for 5-HT (yellow arrows).

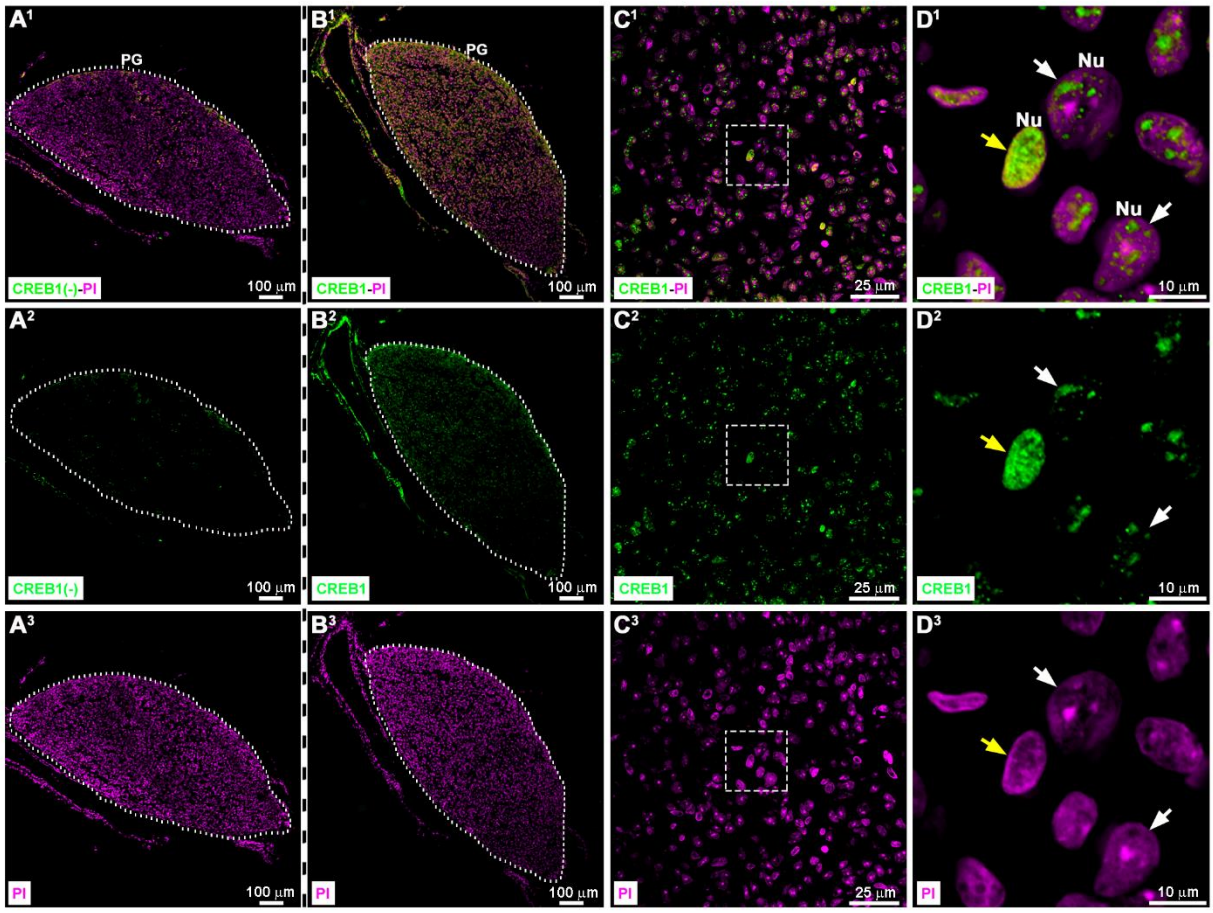

Fig. S2. Heterogeneous distribution of CREB1 among the different cell types within the rat pineal gland.

Section of an adult pineal gland (PG) collected at ZT14 and immunolabeled for CREB1 (green). Cell nuclei (Nu) were stained with propidium iodide (PI; magenta). (A^1-A^3) Negative control by omission of the anti-CREB1 antibody. (B^1-D^3) PG section in the presence of the primary antibody and/or the nuclear dye. (A^1-B^3) 10x images; scale bar: 100 µm. The PG perimeter is defined by a dashed white line. (C^1-C^3) 60x images; scale bar: 25 µm. (D^1-D^3) 5x digital zooms of the insets shown in C^1-C^3; scale bar: 10 µm. CREB1 occupies discrete domains within the nuclei of pinealocytes (white arrows). In contrast, CREB1 is compactly and homogenously distributed in the nucleus of a non-pinealocyte cell (yellow arrow). ZT: Zeitgeber time.

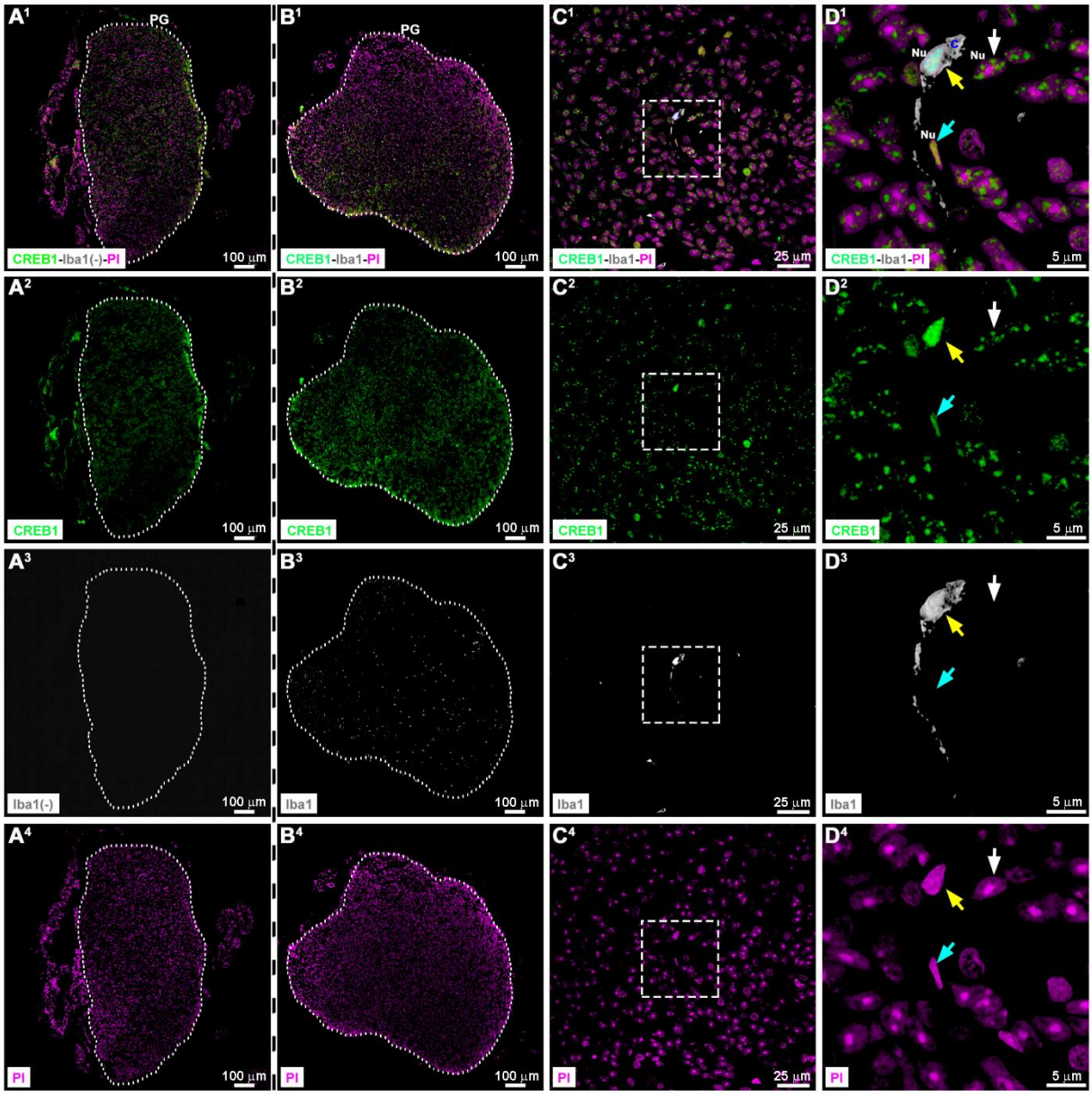

Fig. S3. Homogeneous and dense distribution of CREB1 in the nuclei of phagocytes within the rat pineal gland.

Sections of adult pineal glands (PG) immunolabeled for CREB1 (green) and the microglia/macrophage-specific ionized calcium-binding adapter molecule 1 (Iba1; grey). Nuclei (Nu) were stained with propidium iodide (PI; magenta). (A^1-A^4) Negative control in the absence of the anti-Iba1 antibody. (B^1-D^4) Double immunolabeling of a PG section in the presence of the nuclear dye. Single channels and merged images are shown. (A^1-B^4) 10x images; scale bar: 100 µm. The PG perimeter is defined by a dashed white line. (C^1-C^4) 60x images; scale bar: 25 µm. (D^1-D^4) 2x digital zooms of the insets shown in C^1-C^4; scale bar: 5 µm. CREB1 is present in the nucleus of an Iba1$^+$ cell, with a homogeneous and dense distribution (yellow arrow). A similar compact pattern of CREB1 is observed in an elongated nucleus of a non-pinealocyte cell (cyan arrow). A pinealocyte nucleus with discrete domains of CREB1 is indicated (white arrow). C: cytoplasm.

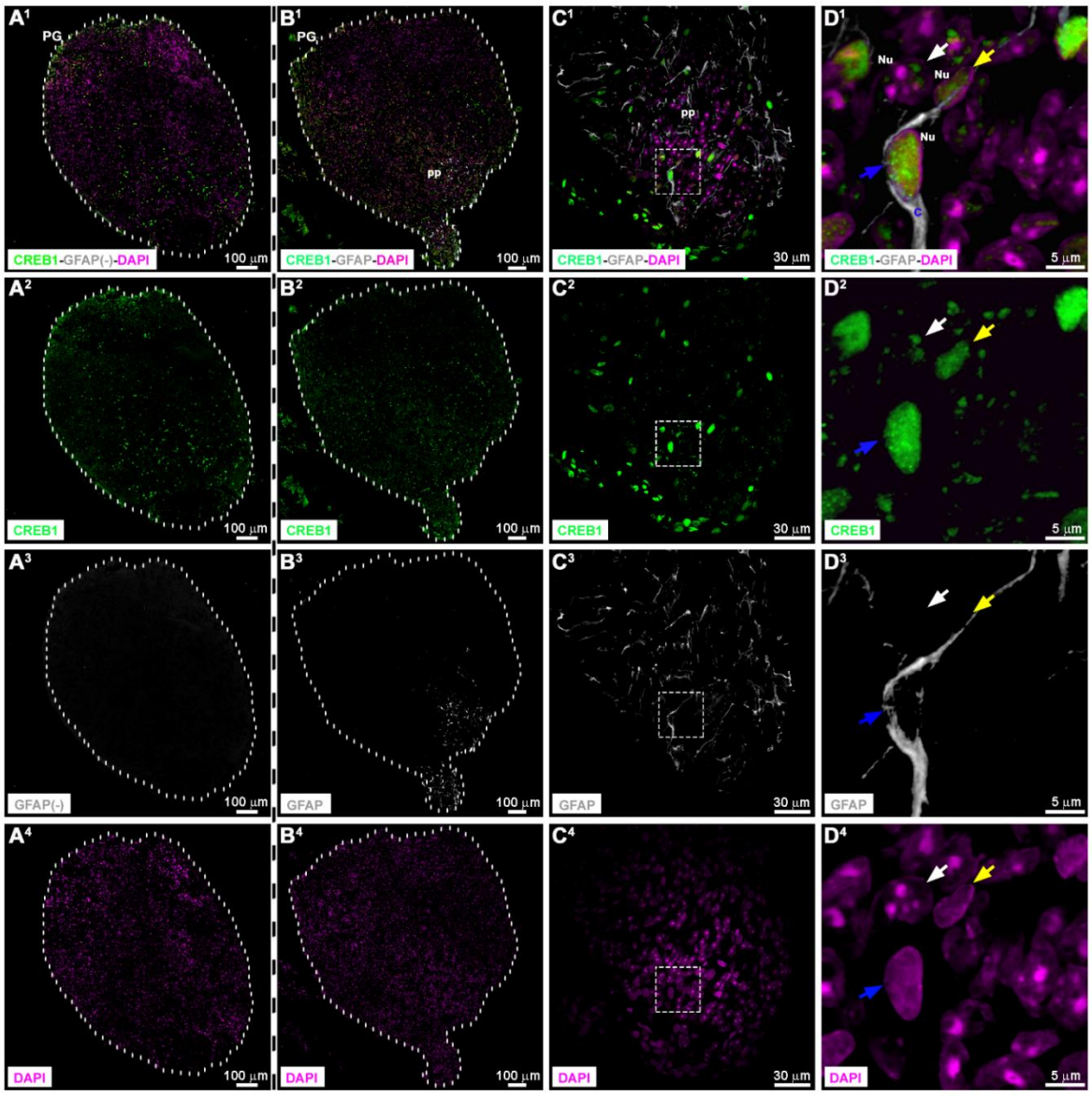

Fig. S4. Homogeneous and dense distribution of CREB1 in the nuclei of astrocytes within the rat pineal gland.

Sections of adult pineal glands (PG) immunolabeled for CREB1 (green), and the glial fibrillary acidic protein (GFAP; grey) which is a marker commonly used for the identification of astrocytes and precursor-like cells. Nuclei (Nu) were stained with 4',6-diamidino-2-phenylindole (DAPI; magenta). (A^1-A^4) Negative control by the omission of the anti-GFAP antibody. (B^1-D^4) Double immunolabeling of a PG section in the presence of DAPI. Single channels and merged images are shown. (A^1-B^4) 10x images; scale bar: 100 µm. The PG perimeter is defined by a dashed white line. (C^1-C^4) 60x images; scale bar: 30 µm. (D^1-D^4) 6.1x digital zooms of the insets shown in C^1-C^4; scale bar: 5 µm. In the proximal pole (pp) of the PG section, CREB1 is present in the nuclei of $GFAP^+$ cells, with a homogeneous and dense distribution (blue arrow). A similar compact pattern of CREB1 is observed in a non-pinealocyte cell, negative for GFAP (yellow arrow). A pinealocyte nucleus with discrete domains of CREB1 is indicated (white arrow). C: cytoplasm.

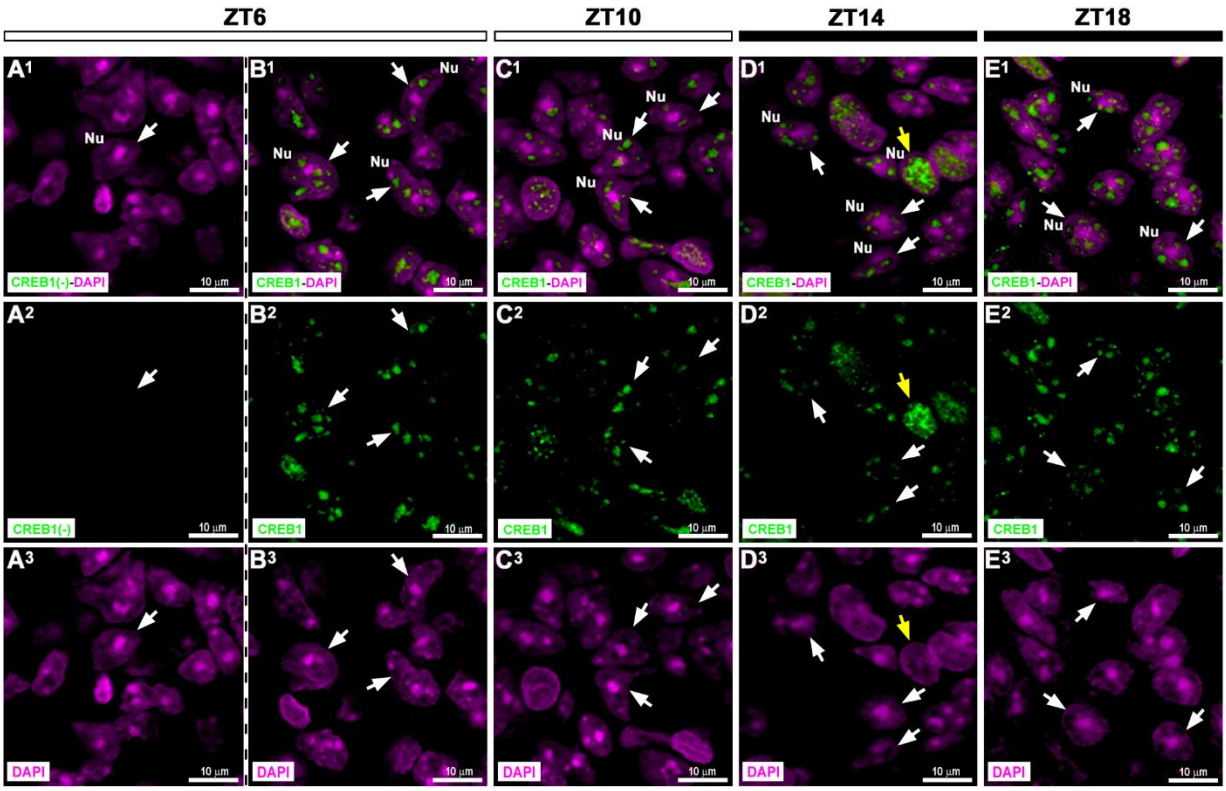

Fig. S5. Heterogenous distribution of CREB1 among rat pinealocyte nuclei.

Sections of adult rat pineal glands (PG) immunolabeled for CREB1 (green). Nuclei (Nu) were stained with 4',6-diamidino-2-phenylindole (DAPI; magenta). (A^1-A^3) Incubation without the anti-CREB1 antibody (negative control). (B^1-E^3) Immunostaining for CREB1 at daytime (ZT6 and ZT10), and at nighttime (ZT14 and ZT18). (A^1-E^3) 2x digital zooms from 60x images; scale bar: 10 µm. Heterogeneity in CREB1 distribution is observed among pinealocyte nuclei (white arrows) at a defined ZT and among ZTs. A non-pinealocyte nucleus, densely immunoreactive for CREB1, is indicated (yellow arrow). ZT: Zeitgeber time.

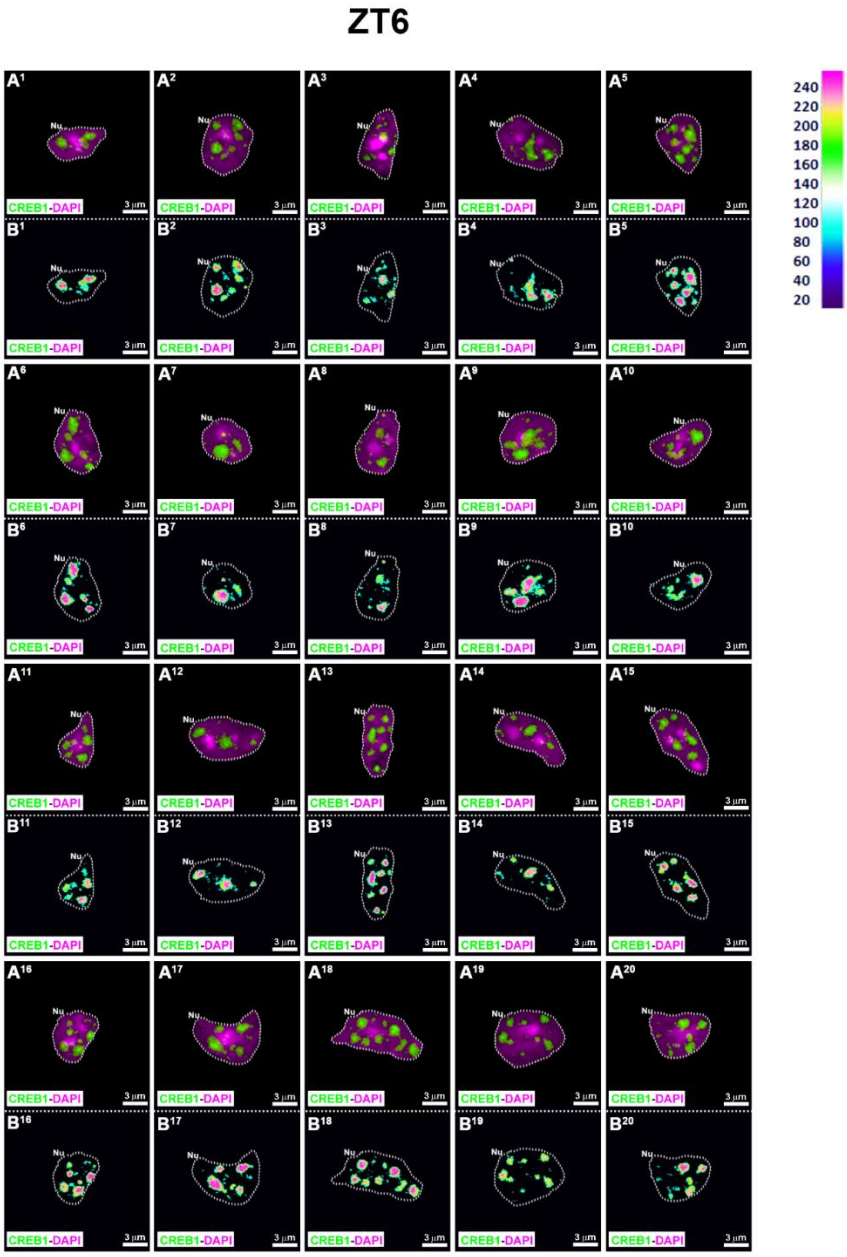

Fig. S6. Spatial distribution of CREB1 within individual pinealocyte nuclei at ZT6.

(A^1-A^{20}) Twenty representative pinealocyte nuclei (Nu), immunolabeled for CREB1 (green), were isolated from pineal gland sections of adult rats sacrificed at ZT6. Nuclei were counterstained with 4',6-diamidino-2-phenylindole (DAPI; magenta). (B^1-B^{20}) Schematic representations of the fluorescence intensity of CREB1 for each pixel within the nuclei shown in A^1-A^{20}. The fluorescence intensity ranges from 0 to 255. To build these representations, the intensity values were look-up table (LUT) mapped to color values using the ImageJ software (Version 1.52d, NIH, USA). (A^1-B^{20}) 2x digital zooms from 60x images; scale bar: 3 µm. Nuclei were selected from 4 pineal glands (PG). The nuclear perimeter is defined by a dashed white line. ZT: Zeitgeber time.

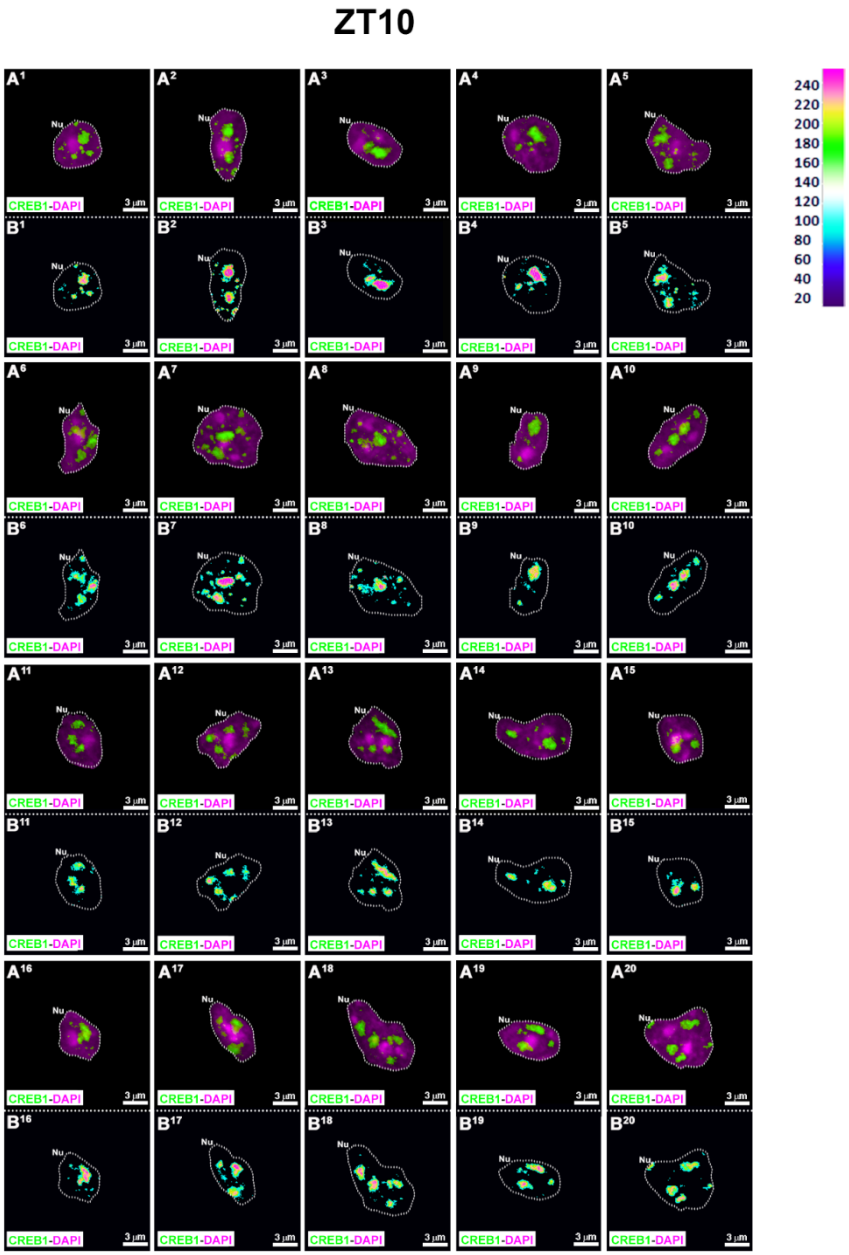

Fig. S7. Spatial distribution of CREB1 within individual pinealocyte nuclei at ZT10.

(A^1-A^{20}) Twenty representative pinealocyte nuclei (Nu), immunolabeled for CREB1 (green), were isolated from pineal gland sections of adult rats sacrificed at ZT10. Nuclei were counterstained with 4',6-diamidino-2-phenylindole (DAPI; magenta). (B^1-B^{20}) Schematic representations of the fluorescence intensity of CREB1 for each pixel within the nuclei shown in A^1-A^{20}. The fluorescence intensity ranges from 0 to 255. (A^1-B^{20}) 2x digital zooms from 60x images; scale bar: 3 µm. Nuclei were selected from 4 pineal glands (PG). The nuclear perimeter is defined by a dashed white line. ZT: Zeitgeber time.

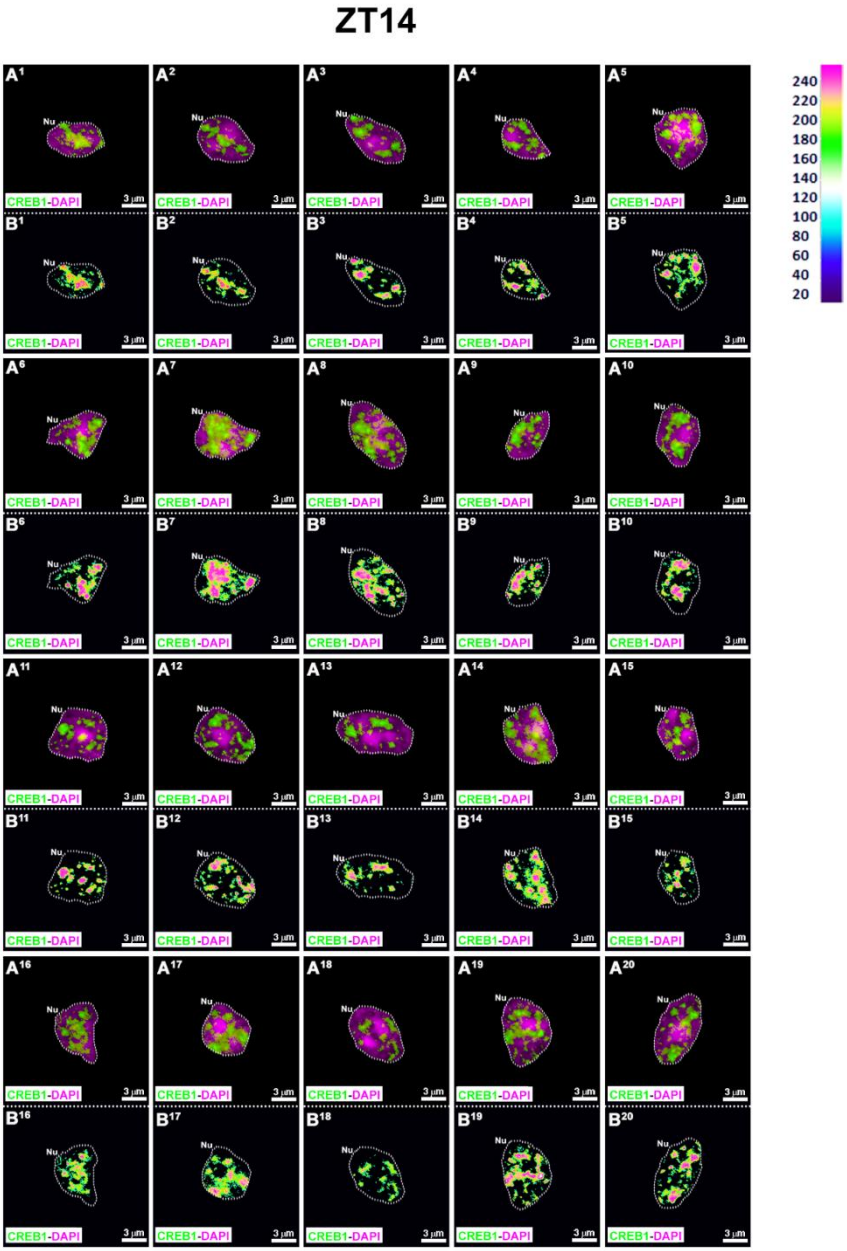

Fig. S8. Spatial distribution of CREB1 within individual pinealocyte nuclei at ZT14.

(A^1-A^{20}) Twenty representative pinealocyte nuclei (Nu), immunolabeled for CREB1 (green), were isolated from pineal gland sections of adult rats sacrificed at ZT14. Nuclei were counterstained with 4',6-diamidino-2-phenylindole (DAPI; magenta). (B^1-B^{20}) Schematic representations of the fluorescence intensity of CREB1 for each pixel within the nuclei shown in A^1-A^{20}. The fluorescence intensity ranges from 0 to 255. (A^1-B^{20}) 2x digital zooms from 60x images; scale bar: 3 µm. Nuclei were selected from 3 pineal glands (PG). The nuclear perimeter is defined by a dashed white line. ZT: Zeitgeber time.

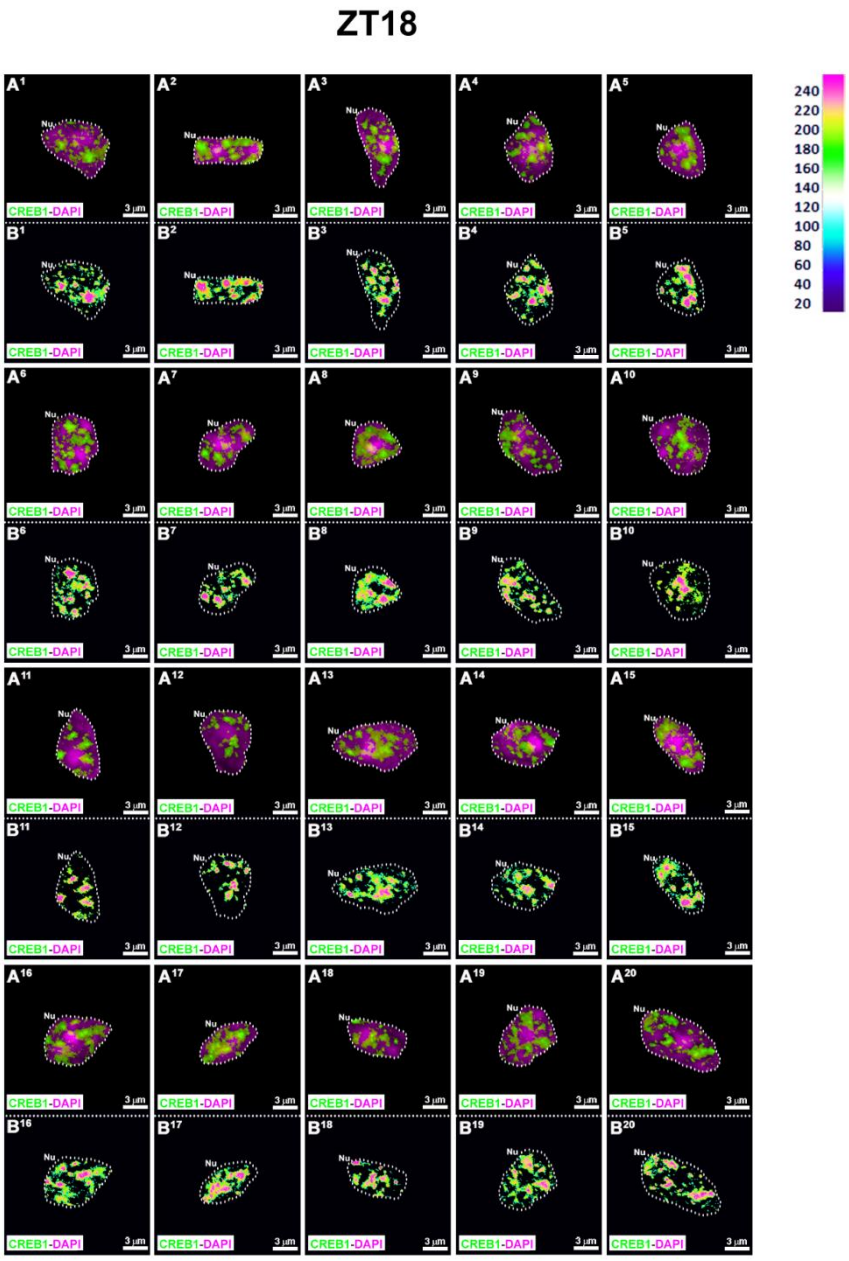

Fig. S9. Spatial distribution of CREB1 within individual pinealocyte nuclei at ZT18.

(A^1-A^{20}) Twenty representative pinealocyte nuclei (Nu), immunolabeled for CREB1 (green), were isolated from pineal gland sections of adult rats sacrificed at ZT18. Nuclei were counterstained with 4',6-diamidino-2-phenylindole (DAPI; magenta). (B^1-B^{20}) Schematic representations of the fluorescence intensity of CREB1 for each pixel within the nuclei shown in A^1-A^{20}. The fluorescence intensity ranges from 0 to 255. (A^1-B^{20}) 2x digital zooms from 60x images; scale bar: 3 µm. Nuclei were selected from 3 pineal glands (PG). The nuclear perimeter is defined by a dashed white line. ZT: Zeitgeber time.

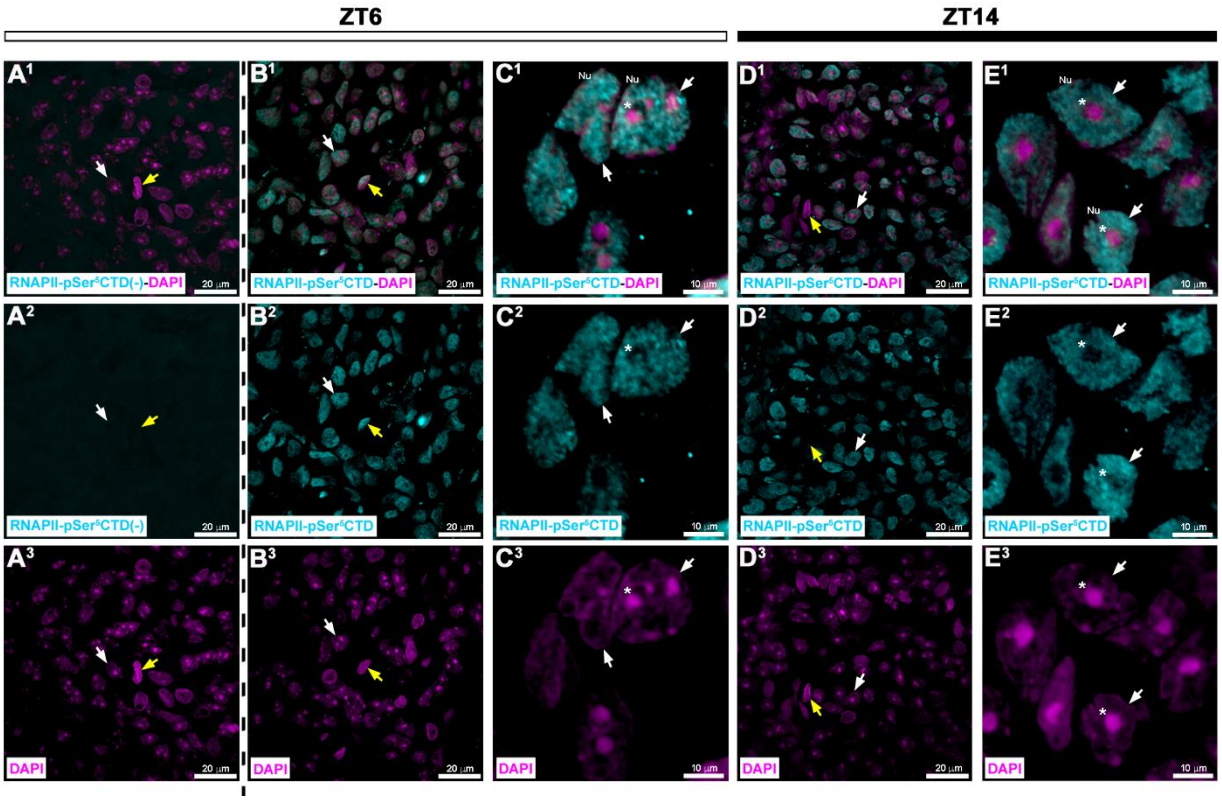

Fig. S10. Day/night analysis of the nuclear distribution of the phosphorylated RNA polymerase II in the rat pineal gland.

Sections of adult rat pineal glands collected during the daytime (ZT6) and nighttime (ZT14), immunolabeled for a particular phosphorylated form of the RNA polymerase II (RNAPII-pSer^{5}CTD; cyan). Nuclei (Nu) were counterstained with 4',6-diamidino-2-phenylindole (DAPI; magenta). (A^1-A^3) Negative control by omission of the anti-RNAPII-pSer^{5}CTD antibody. (B^1-E^3) Single channels and merged images are shown. (A^1-A^3, B^1-B^3, D^1-D^3) 60x images; scale bar: 20 µm. (C^1-C^3, E^1-E^3) 10x digital zooms from 60x images; scale bar: 5 µm. Pinealocyte nuclei immunoreactive for RNAPII-pSer^{5}CTD are indicated (white arrows). Non-pinealocyte nuclei with different levels of RNAPII-pSer^{5}CTD are also indicated (yellow arrows). Asterisks: nucleoli without RNAPII-pSer^{5}CTD signal, present within pinealocyte nuclei. CTD: C-terminal repeat domain (YSPTSPS) of the RNA polymerase II.

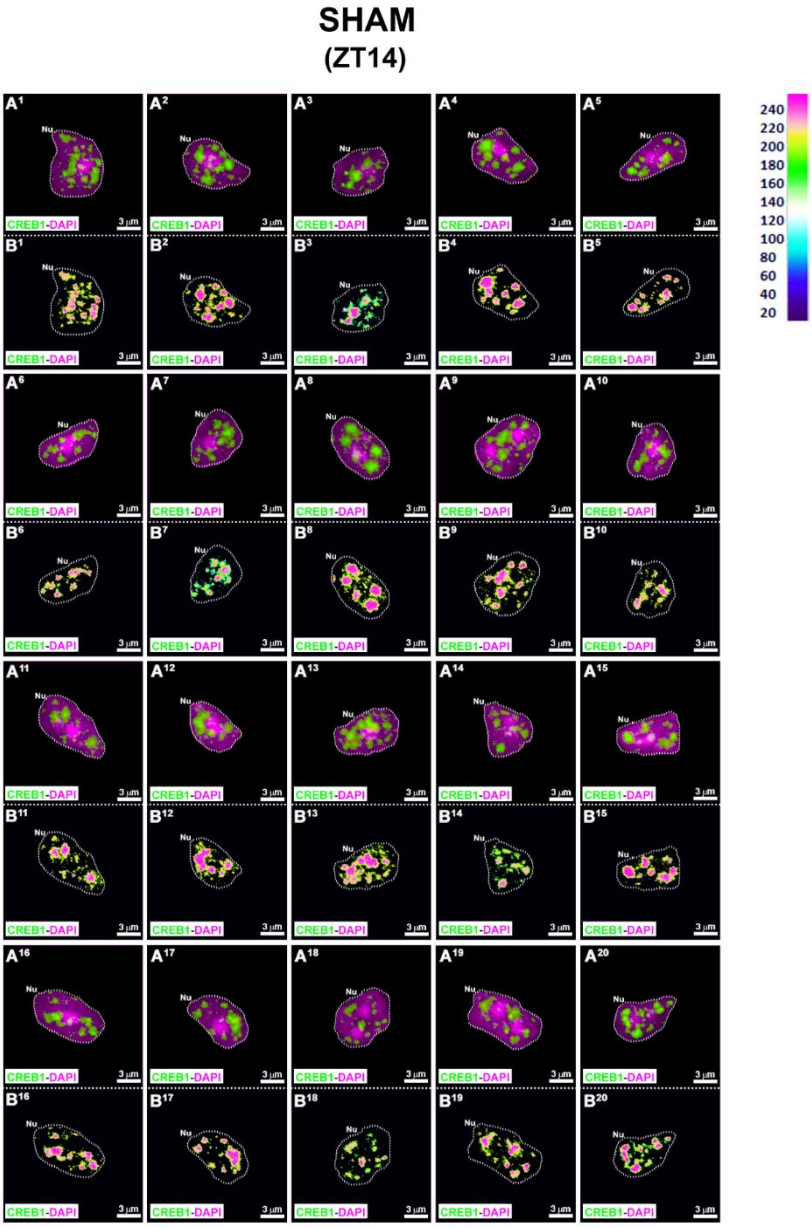

Fig. S11. Spatial distribution of CREB1 within individual pinealocyte nuclei of adult sham-operated rats.

(A^1-A^{20}) Twenty representative pinealocyte nuclei (Nu), immunoreactive for CREB1 (green), were isolated from pineal gland sections of adult sham-operated rats sacrificed three weeks after surgery at ZT14 (N=4). Nuclei were stained with 4',6-diamidino-2-phenylindole (DAPI; magenta). The fluorescence intensity ranges from 0 to 255. (B^1-B^{20}) Schematic representations of the fluorescence intensity of CREB1 for each pixel within the nuclei shown in A^1-A^{20}. (A^1-B^{20}) 2x digital zooms from 60x images; scale bar: 3 µm. The nuclear perimeter is defined by a dashed white line. ZT: Zeitgeber time.

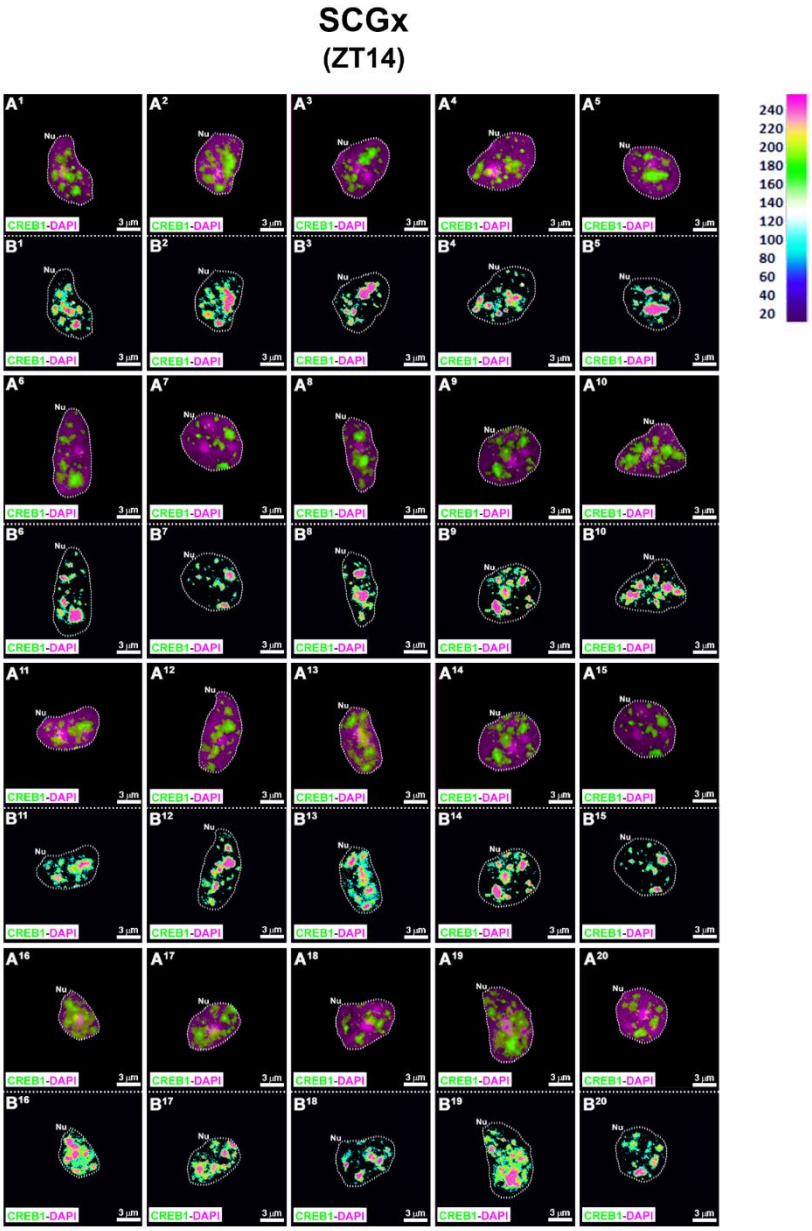

Fig. S12. Spatial distribution of CREB1 within individual pinealocyte nuclei at ZT14, after chronic bilateral superior cervical ganglionectomy.

Spatial distribution of CREB1 within individual pinealocyte nuclei at ZT14, after chronic bilateral superior cervical ganglionectomy. (A^1-A^{20}) Twenty representative pinealocyte nuclei (Nu), immunoreactive for CREB1 (green), were isolated from pineal gland sections of adult SCGx rats sacrificed three weeks after surgery at ZT14 (N=4). Nuclei were stained with 4',6-diamidino-2-phenylindole (DAPI; magenta). (B1-B^{20}) Schematic representations of the fluorescence intensity of CREB1 for each pixel within the nuclei shown in A^1-A^{20}. The fluorescence intensity ranges from 0 to 255. (A^1-B^{20}) 2x digital zooms from 60x images; scale bar: 3 µm. The nuclear perimeter is defined by a dashed white line. SCGx: superior cervical ganglionectomy; ZT: Zeitgeber time.

Please cite this paper as:
Farias Altamirano, L.E., Vásquez, E., Freites, C.L., Ibañez, J.E., Guido, M.E. and Muñoz, E.M. 2023. CREB1 spatio-temporal dynamics within the rat pineal gland. Melatonin Research. 6, 3 (Sep. 2023), 234-255. DOI:https://doi.org/https://doi.org/10.32794/mr112500153